7.4 THE SPECTRAL COMPOSITION OF FLUXES AND VARIANCES OVER LAND AND SEA

Donald H. Lenschow*, and Jielun Sun

National Center for Atmospheric Research, Boulder, CO

1. INTRODUCTION

Measuring contributions to variances and fluxes as a function of wavenumber in the convective planetary boundary layer (PBL) using instrumented aircraft has become commonplace [e.g. Lenschow (1986); Oncley et al. (1997)]. Generally, the spectral region of interest extends from wavenumbers of order 0.1 cycles km^{-1} (i.e. scales of several times the depth of the PBL) to about 10^2 cycles km^{-1}. This is the wavenumber region that contains most of the flux. However, this may not always be the case, as there is no a priori reason for the flux at smaller wavenumbers to always be negligible by comparison. Certainly variances of the horizontal velocity components and scalars are not negligible in this mesoscale wavenumber region. Here we consider "mesoscale" as variations on a horizontal scale of from several times the PBL depth, i.e. ≥ 10 km, to about 100 km. At these small wavenumbers, fixed-point measurements from e.g. towers cannot adequately resolve the spectral structure since the turbulence time scale is too short relative to the advective time scale.

There are several sources of mesoscale variability that are relevant in this context: First, clouds contained within the PBL or originating at the top of the PBL and extending into the free troposphere can generate mesoscale fluctuations both due to shading of the ground (over land), which modulates the surface energy budget, and by dynamical effects resulting from the buoyancy generated by phase changes and by cloud-top radiative cooling. Second, terrain height variations can directly modulate flow patterns on the mesoscale over land. Third, variations in surface properties such as surface roughness (e.g. trees vs. grassland) and surface energy budget (e.g. wet vs. dry soil) can induce flows that scale with the surface heterogeneity. Finally, dynamical atmospheric processes such as longitudinal rolls, mesoscale cellular convection, and gravity waves in the overlying free troposphere can introduce mesoscale variability directly into the PBL flow field.

Here we first consider the limitations on accuracy of air motion measurement from aircraft at mesoscale wavenumbers, since as far as we know, this has not been systematically treated for currently-used systems. We assume that an inertial reference system (IRS) is used to obtain the airplane horizontal velocity components and attitude angles. We then show averaged spectra and cospectra from measurements obtained with the NCAR Electra aircraft over the boreal forest of Canada during the summer of 1994 as a contribution to the BOreal Ecosystem-Atmosphere Study (BOREAS), and over the western equatorial Pacific Ocean from the Tropical Ocean Global Atmosphere Coupled Ocean-Atmosphere Response Experiment (TOGA COARE) between 15 November 1992 and 17 January 1993 (Sun et al., 1996). We do not attempt to normalize the observations with e.g. mixed-layer similarity parameters since our focus is on the mesoscale, where appropriate scaling variables are not known, and furthermore mixed-layer scaling parameters are not available in all cases.

2. MEASUREMENT ACCURACY

We first consider errors in the vertical air velocity component w since its mesoscale fluctuation level is considerably smaller that the alongwind u and crosswind v fluctuations due to being constrained by the underlying surface and the capping BL inversion.

As we show in Fig. 1, the magnitude of mesoscale fluctuations (wavenumber $k < 10^{-1}$ cycles km^{-1}) in the vertical air velocity component w measured by the Electra in TOGA COARE (which has a smaller fluctuation level than BOREAS) is $\sigma_{wm} \simeq 0.1$ m s^{-1}. We conservatively assume that the minimum signal level needed to accurately measure such a signal is 20% of this and that the entire contribution to the signal is at $k = 10^{-2}$ cycles km^{-1}. The limiting error for mesoscale measurement is likely to be drift in the sensor outputs used to measure w. This means that for an airplane true airspeed of $\mathcal{U} \sim 100$ m s^{-1},

$$\frac{\partial w}{\partial t} < 2 \times 10^{-4} \text{ m s}^{-2} \qquad (1)$$

Lenschow (1986) shows that the following approximate relation is adequate for consideration of errors in aircraft

*corresponding author address: Donald H. Lenschow, National Center for Atmospheric Research, P. O. Box 3000, Boulder, CO 80307-3000; email: lenschow@ucar.edu

w measurements:

$$w \simeq \mathcal{U} \sin\Theta + w_p, \tag{2}$$

where

$$\Theta \equiv \text{attack angle} - \text{pitch angle} = \alpha - \theta, \tag{3}$$

and w_p is the airplane vertical velocity. The attack angle is the angle of the airflow relative to the aircraft in the vertical plane of the aircraft and the pitch angle is the angle of the longitudinal axis of the aircraft relative to the local horizontal plane of the earth. Both of these angles are typically $< \pm 5^\circ$ for normal research legs, so we make the further approximation in (2) that

$$w \simeq \mathcal{U}\Theta + w_p. \tag{4}$$

For evaluating errors, we differentiate (4) with time and equate it to (1),

$$\frac{\partial w}{\partial t} \simeq \Theta\frac{\partial \mathcal{U}}{\partial t} + \mathcal{U}\frac{\partial \Theta}{\partial t} + \frac{\partial w_p}{\partial t} \leq 10^{-4} \text{ m s}^{-2} \tag{5}$$

Dynamic pressure from a Pitot tube q is used, along with static pressure P and temperature T, to obtain the true airspeed via the relation,

$$\mathcal{U} \simeq \sqrt{\frac{2qRT}{P}}, \tag{6}$$

where R is the gas constant. We assume a pressure measurement accuracy of 0.7 hPa over a nominal 6 hour flight at 100 m s^{-1} (e.g. Khelif et al. (1999); NCAR (1991)). The value of Θ will seldom exceed $\pm 2^\circ$. Using these values for the first term in (5) gives

$$\Theta\frac{\partial \mathcal{U}}{\partial t} \leq 10^{-6} \text{ m s}^{-2}. \tag{7}$$

Considering the second term in (5), the error in Θ may contain errors in both the attack angle and the pitch angle, each of which is measured by entirely different technologies. The pitch angle is typically measured with an IRS or with an instrument utilizing the Global Positioning System (GPS). The IRS maintains an Earth-based coordinate system (either mechanically or computationally) using gyroscopes to maintain an absolute earth-based reference for the attitude angles of the aircraft, and the doubly-integrated output of accelerometers to continuously calculate its position. As the position of the aircraft changes, its angular orientation with respect to the local earth also changes. This means that the IRS must continuously update its local orientation so that the gravitational acceleration g is not included in the computation of the updated position from the integrated accelerations. GPS is a satellite-based radio navigation system which measures attitude angles from relative differences in the absolute position of a set of radio receivers, which are mounted some distance apart.

The primary limitation in pitch angle accuracy from IRS is the error contribution from the Schuler oscillation, whose frequency is given by

$$\omega_s = \sqrt{\frac{g}{R}} \simeq 1.24 \times 10^{-3} \text{ rad s}^{-1}, \tag{8}$$

where R is the radius of the Earth and g is gravity. This ~ 84.4 minute oscillation can result from a displacement or perturbation in θ which introduces an erroneous contribution to the horizontal acceleration from g. When integrated, this error acceleration rotates the angular reference of the IRS in an undamped periodic oscillation about a zero mean.

For an IRS with an overall navigational accuracy of $\sim$ 3 km hr^{-1}, the angular stability of the platform (Britting, 1971) is

$$\frac{\partial \theta}{\partial t} < 6 \times 10^{-5}\omega_s \text{ rad s}^{-1} \simeq 3 \times 10^{-7} \text{ rad s}^{-1}. \tag{9}$$

This is in reasonable agreement with the overall pitch angle accuracy specified for the currently-used Honeywell Laseref SM IRS, $\pm 0.05^\circ$ over 6 hours duration (NCAR, 2003) if we assume that this error is modulated at the Schuler frequency. Thus, the pitch error contribution to the second term on the right side of (5) is

$$\mathcal{U}\frac{\partial \theta}{\partial t} \leq 2 \times 10^{-5}. \tag{10}$$

Therefore, we conclude that the IRS is inherently capable of measuring pitch to sufficient accuracy for measuring mesoscale vertical motions.

Attack angle is measured by means of flow angle sensors mounted on or near the nose of the aircraft. Most commonly, the flow angle is obtained from pressure difference measurements δP between a set of ports either located directly on the nose of the aircraft (radome technique; see e.g. Brown et al. (1983)), or on a probe mounted near the front of the aircraft (e.g. Williams et al. (1996)), usually on a boom projecting forward of the aircraft nose (e.g. Khelif et al. (1999)). It is difficult to quantify the drift that may occur in this measurement, but we proceed as follows: We use a typical differential pressure sensitivity factor of $\kappa = 6.5$ (deg.)$^{-1}$ (Brown et al., 1983), where κ is defined by the relation

$$\delta\alpha \equiv \frac{1}{\kappa}\frac{\delta P}{q} \tag{11}$$

and q is the dynamic pressure (~ 60 hPa at $\mathcal{U} = 100$ m s^{-1}). We need to be able to measure differential pressure with a long-term drift of ≤ 4.8 hPa over a period of

6 hours, or alternatively, a short-term drift of ≤ 0.1 hPa over 8 minutes in order to achieve the drift rate accuracy given in (1). The transducers used for this measurement by the NCAR Research Aviation Facility (NCAR, 1991) have an overall accuracy of 0.2 hPa, but this includes several long-term sources of error such as calibration errors, turn-on to turn-on differences, and temperature changes over the entire operating range of the transducers. Thus, we conclude that current differential pressure transducers are sufficiently accurate for mesoscale measurements of w.

There may, however, be other sources of drift in this term such as changes in the mean attack angle due to fuel burn-off or systematic airspeed changes which, combined with undocumented flow distortion effects, may contribute significantly to the drift. For the short-term drift example given above, the allowable drift is only about 0.16% of the total dynamic pressure. This issue remains an open question worthy of further investigation.

The required vertical acceleration accuracy of $\partial w_p/\partial t < 2\times10^{-4}$ m s^{-2} requires external information, since the vertical acceleration is not contained within a periodic oscillation. Doubly integrating an erroneous acceleration in the vertical direction leads to a parabolic increase in vertical position error (e.g. Lenschow (1972), Lenschow and Spyers-Duran (1989)). Thus, external information is needed to limit vertical position error. The value of g decreases with altitude by about 3×10^{-5}s^{-2}. Thus to measure g to the required accuracy would require absolute height measurement to 3 m accuracy over the period of measurement ($\sim$ 100 to 1000 s). This is difficult in practice. Neither standard GPS- nor geometric-determined altitude are generally this accurate. Furthermore, using geometric altimeters for absolute altitude requires determination of the surface elevation to the same accuracy, which is feasible over the ocean, but difficult over land.

The standard way for measuring height is by means of static pressure measurement. To meet this accuracy limit, assuming the pressure measurement itself is sufficiently accurate, the pressure gradient must be ≤ 0.3 Pa m^{-1} (3 hPa/1000 km), which is usually the case in practice, except near strong cyclonic disturbances or deep convection, or in orographic flow.

In contrast to w, the spectra (times wavenumber) for along- and crosswind horizontal components u and v are approximately flat (for BOREAS) or increase somewhat (for TOGA COARE) for decreasing wavenumber. Thus, at a wavenumber of 10^{-2} cycle km^{-1}, the u,v spectra are roughly a factor of 100 larger than the w spectrum, so the accuracy criteria are not nearly so stringent. Since both horizontal wind component spectra are approximately the same magnitude, for convenience in estimating measurement errors, we consider the air velocity measurements in the aircraft coordinate system. Carrying out an analysis using the approximate equations presented e.g. in Lenschow (1986) or Lenschow and Spyers-Duran (1989) rotated to the aircraft coordinate system with approximations similar to (3),

$$u_x \simeq -\mathcal{U} + u_{px} \tag{12}$$

$$v_y \simeq \simeq \mathcal{U}\Psi + v_{py}, \tag{13}$$

where (u_x, v_y) are the longitudinal (along the airplane axis) and lateral (normal to the airplane axis) wind components, respectively,

$$\Psi \equiv \psi' + \beta, \tag{14}$$

where ψ' is the departure of the measured true heading from the actual true heading, β is the sideslip angle (i.e. the airflow angle in the horizontal plane of the aircraft), and (u_{px}, v_{py}) are the longitudinal and lateral airplane velocity components.

Taking the time derivatives of (12) and (13), we obtain

$$\frac{\partial u_x}{\partial t} \simeq -\frac{\partial \mathcal{U}}{\partial t} + \frac{\partial u_{px}}{\partial t} \tag{15}$$

$$\frac{\partial u_y}{\partial t} \simeq \Psi\frac{\partial \mathcal{U}}{\partial t} + \mathcal{U}\frac{\partial \Psi}{\partial t} + \frac{\partial v_{py}}{\partial t}. \tag{16}$$

Again considering mesoscale fluctuations; i.e. $k < 10^{-2}$ cycles km^{-1}, the standard deviation of the horizontal components (Fig. 1) for both BOREAS and TOGA COARE is $\sigma_{um} \simeq \sigma_{vm} \simeq 1$ m s^{-1}. We again conservatively assume that the entire contribution to the mesoscale signal is at 10^{-2} cycles km^{-1} and that we need to measure to 20% of the measured signal. The required accuracy for mesoscale measurement is

$$\frac{\partial u_x}{\partial t} \simeq \frac{\partial v_y}{\partial t} \leq 2\times10^{-3} \text{ m s}^{-2}. \tag{17}$$

Evaluating the first term on the right side of (15) using the same Pitot pressure accuracy as was used to estimate the first term in (5) of 0.7 hPa over 6 hours at 100 m s^{-1}, we obtain

$$\frac{\partial \mathcal{U}}{\partial t} = 2.7\times10^{-5} \text{ m s}^{-2}. \tag{18}$$

The second term in (15) and third term in (16) can be estimated from the expected contribution from the Schuler oscillation (8) of the IRS. For a 1 m s^{-1} oscillation, we have

$$\frac{\partial u_{px}}{\partial t} \simeq \frac{\partial v_{py}}{\partial t} \simeq 1.3\times10^{-3} \text{ m s}^{-2}. \tag{19}$$

This is also less than required for resolving the observed mesoscale motions. Furthermore, this can be decreased even more by GPS updating of the horizontal velocity components.

The first term in (16) can be evaluated similar to the first term in (5), with the result that

$$\Psi \frac{\partial u}{\partial t} \leq 10^{-6} \text{ m s}^{-2}. \quad (20)$$

The second term in (16) can be evaluated similar to the second term in (5); however, the IRS true heading measurement is less accurate than the pitch angle measurement since it is not directly constrained by the Schuler oscillation loop. From the analysis of Britting (1971), the inherent IRS accuracy of currently deployed systems gives a drift rate of

$$u \frac{\partial \psi'}{\partial t} \leq 10^{-4} \text{ m s}^{-2}. \quad (21)$$

Since the sideslip angle is measured with the same technique as the attack angle, its drift rate is also similar. The accuracy requirement for u and v, however, is an order of magnitude less that for w, so its contribution to the drift error is proportionately smaller. Thus, all the terms in (15) and (16) are small compared to observed mesoscale horizontal velocity variations.

To summarize, we conclude that the observed spectra of w are within the envelope of the estimated measurement accuracies, and that the attack angle measurement is likely the weakest link. The observed u and v spectra are similarly within the envelope of the estimated measurement accuracies, with the true heading drift rate as possibly the weakest link.

3. MEASUREMENT RESULTS

Our data base for measurements over land is from the NCAR Electra flights in the convective PBL that traversed large sections of the boreal forest of Canada during BOREAS. The location and times of the flight legs are given by Oncley et al. (1997), and a brief description of the instrumentation used here by Dobosy et al. (1997). The flights were centered about mid-day throughout the summer, with clear to partly cloudy (mostly fair-weather cumulus) conditions at a height of $\sim$ 100 m above the surface. The 31 legs used here varied from 228 to 666 km in length (38 to 111 minutes). The average height of the PBL was $z_i \simeq 1300$ m. The terrain varied from flat to rolling hills, and from solid forest to subarctic tundra, with about 10% of the tracks over lakes. There very little evidence of any direct anthropogenic impact on the surface vegetation; the tracks were almost completely north and east of the agricultural limit, and evidence of lumbering was minimal. Therefore, we can consider this data set as representing atmospheric forcing by interaction with a natural surface unaffected by e.g. farming, ranching, lumbering, or urbanization.

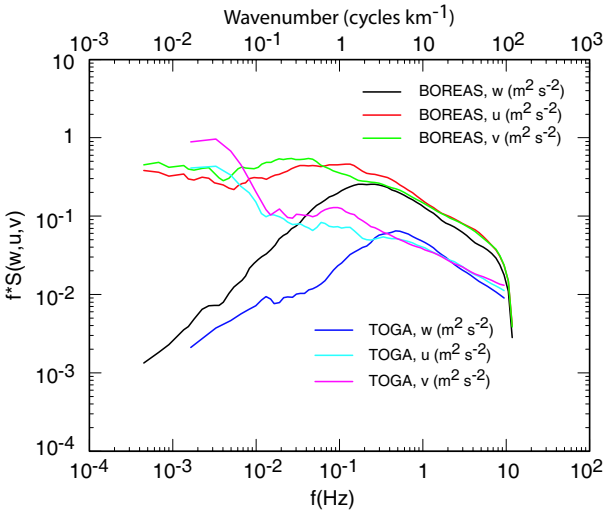

Figure 1: Spectra of the three velocity components for NCAR Electra flights in BOREAS and TOGA COARE.

We compare these results with measurements from the Electra carried out in the equatorial western Pacific PBL during TOGA COARE. The data set used here is described by Sun et al. (1996) who previously had partitioned the eddy fluxes into "turbulent," "large-eddy," and "mesoscale." fluxes. 26 flight legs ranging between 60 km and 120 km in length and 30 m to 40 m altitude are used here for the analysis. Johnson et al. (2001) estimated an average value of $z_i = 512$ m from TOGA COARE sounding data.

Since both examples come from the same aircraft using the same system, any contributions to systematic errors should be similar for both field studies, which adds confidence to the significance of differences in spectra and cospectra between the two studies.

3.1 Spectra

Figure 1 shows plots of spectra times frequency $f \cdot S(f)$ (spectra times wavenumber $k \cdot S(k)$ using the top axis) for the three velocity components. With the exception of the v component in TOGA COARE, the velocity components all have a -2/3 slope in the inertial subrange out to a wavenumber of nearly 100 cycles km^{-1}, where filtering of the raw data results in a more rapid drop-off with wavenumber. (Since the horizontal components are defined with respect to the wind direction, here we do not investigate whether the ratios of the components transverse to the airplane flight track to the along-track component have the predicted 4/3 ratio in the inertial subrange.) The v spectra for TOGA COARE are somewhat flatter than -2/3. At low wavenumbers, i.e. wavenumbers below about 1 cycle km^{-1}, the BOREAS u and v spectra

flatten out, while the w spectra have a +1 slope. Thus if we had not multiplied the spectra by wavenumber, the u and v spectra would have a -1 slope and the w spectra would be flat in this region.

The peak in $S_w(k)$ is at smaller wavenumbers for the BOREAS spectrum than for the TOGA COARE spectrum, both as a consequence of the greater PBL depth and the higher flight level. This also similarly affects the cospectral peaks. The horizontal velocity spectra are known to be little affected by this difference in flight level (Kaimal and Finnigan, 1994).

In the inertial subrange, the TOGA COARE spectra are a factor of about 3 smaller than the overland spectra. This is a direct result of the considerably smaller surface buoyancy flux over the ocean. However, the u and v spectra over the ocean cross over at wavenumbers less than about 10 cycles km^{-1}. That is, at very low wavenumbers, there is more variability in the horizontal wind field over the ocean than over land. At first glance this seems surprising, since the land surface is more heterogeneous. This suggests that this is due to large-scale moist convective processes occurring over the tropical ocean, in contrast to the temperate PBL over land. Thus the relatively large contributions at smaller wavenumbers may result not so much from horizontal heterogeneity at the surface as from mesoscale processes in the atmosphere.

Boundary-layer scaling is expected to apply in the region around $k = z_i^{-1} \sim 1$ cycle km^{-1}. That is, we expect that turbulence energy generated by surface buoyancy flux over a horizontally homogeneous surface should occur in this region, and that the turbulence at higher wavenumbers is due to the cascade of turbulence from the energy-containing range to the inertial subrange. This coincides with the region where the velocity spectra start to depart from their low-wavenumber slopes. Thus comparing the contributions at lower wavenumbers to those around $k = z_i^{-1} \sim 1$ km^{-1} gives us a way to estimate the relative contributions of mesoscale variations to those that scale with z_i.

In contrast to the velocity spectra, the scalar spectra from BOREAS, which includes temperature T, humidity q, carbon dioxide s_c, and ozone s_{oz} from the BOREAS flights (Fig. 2) show a flattening in the region around 0.5 to 5 cycles km^{-1}, then a sharp rise in magnitude going to lower wavenumbers. Thus, the relative contribution of the mesoscale to scalar spectra is considerably larger than for u and v (i.e. somewhat more than a factor of 10). We also note that only temperature shows a -2/3 spectrum in the inertial subrange. The three species measurements contain significant noise in this region, but this does not affect their mesoscale variance (nor their cospectra with w).

Comparing the BOREAS and TOGA COARE spectra for temperature and humidity, we see in Fig. 3 that

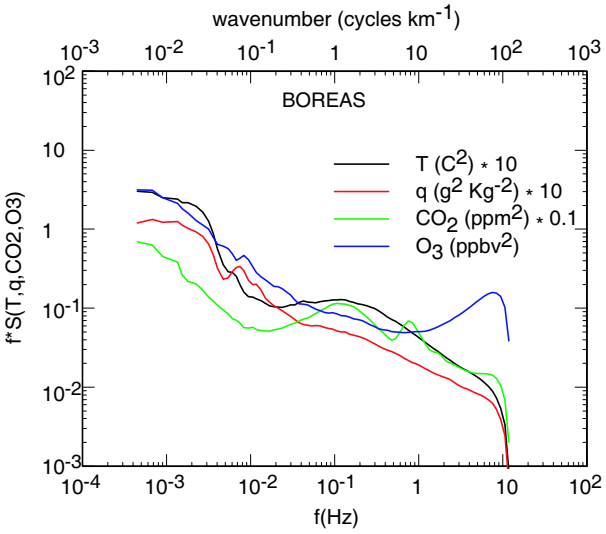

Figure 2: Spectra of temperature, humidity, carbon dioxide and ozone for NCAR Electra flights in BOREAS.

the temperature spectra over land are about 3 to 8 times larger than over the ocean in the inertial subrange. This is not surprising based on the considerably larger temperature flux over land as compared to over the ocean. Surprisingly, at low wavenumbers, there is no significant difference. This suggests that the temperature fluctuations on the mesoscale are not driven by the surface temperature flux. In contrast, the humidity spectra are about the same over the land as over the ocean over the entire spectrum. The Electra TOGA COARE q spectrum contains too much noise to be useful, except at very small wavenumbers, where it agrees with the BOREAS spectrum. In contrast to u and v spectra, T and q spectra do not flatten out for $k \ll 1$ km^{-1}. Instead, they continue to increase by roughly another decade at smaller wavenumbers. That is, these scalar variables have considerably more mesoscale variability, compared to their inertial subrange variance, than u and v. The T spectrum from BOREAS flattens out in the region $0.1 < k < 1$ km^{-1}, but then increases for smaller k, again suggesting that mesoscale temperature fluctuations result from something other than surface temperature flux.

3.2 Cospectra

We now examine the cospectra of w with both u and v, as well as the scalar variables. Figure 4 shows that for the BOREAS data, the cospectrum of u has a large negative peak at about 1 cycle km^{-1}. The v spectrum has a positive peak at about 0.3 cycles km^{-1}. This positive peak is a reflection of the veering, or clockwise rotation of the wind with height. This means that on the average, negative fluctuations of v are transported downward

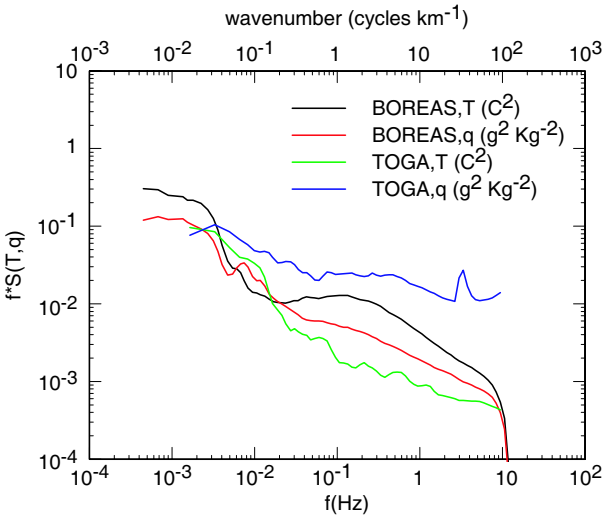

Figure 3: Spectra of temperature and humidity for NCAR Electra flights in BOREAS and TOGA COARE.

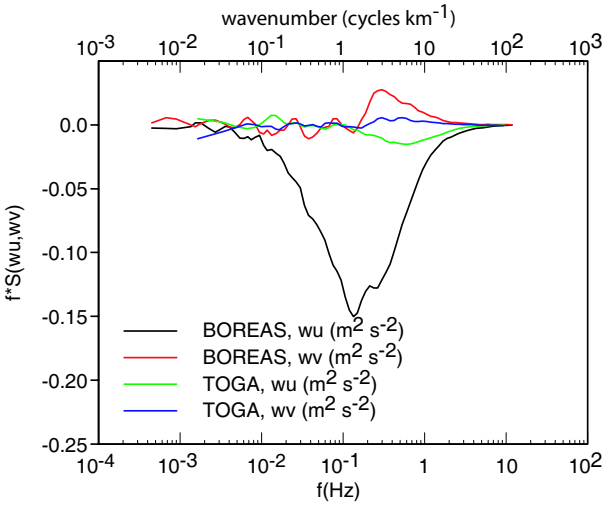

Figure 4: Cospectra of the two vertical momentum flux components from BOREAS and TOGA COARE.

and positive fluctuations upwards. This is consistent with clockwise rotation of the wind with height due to surface friction, so that near the surface v should be greater than higher up. For the TOGA COARE data, both u and v cospectra are small, but show similar behavior. The higher peak wavenumber for v is likely due to upward momentum transport of the v component being dominant while downward transport of v momentum being either negligible or negative, in contrast to u transport which is likely significant (and the same sign) for both upward and downward transport. Since upward transport occurs at smaller scales, this leads to a higher wavenumber peak in the wv cospectra. The oceanic cospectra show similar structure, but much smaller magnitude, reflecting the smoother surface and generally lighter winds. Furthermore, the peak in the v cospectrum, which is so noticeable in the BOREAS results, is very much reduced, as expected because of the smaller Coriolis effect at equatorial latitudes.

The T and q cospectra, shown in Fig. 5 are very similar to each other, and to their corresponding u cospectra. Thus, the differences between the spectra of the scalars and the spectra of u do not lead to any significant differences in their respective cospectra. That is, the enhanced mesoscale contributions to the scalar spectra do not have a noticeable impact on the cospectra.

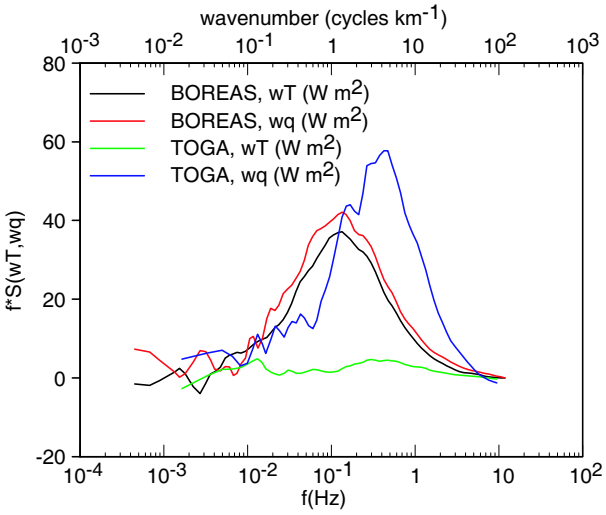

Figure 5: Cospectra of temperature and humidity versus w from BOREAS and TOGA COARE.

4. CONCLUSIONS

We have shown that currently-used IRS-based air motion systems on e.g. the NCAR Electra aircraft can measure mesoscale variations (out to wavenumbers $< 10^{-2}$ cycles km^{-1}) of the three wind components in the con-

vective PBL over both land and sea. We then present summary spectra and cospectra from experiments over the boreal forest of Canada (BOREAS) and over the equatorial western Pacific Ocean (TOGA COARE). The land measurements were obtained at a height of ~ 100 m above the surface and the sea measurements at a height of 30 to 40 m. The results provide a basis for specifying typical levels of scale-resolved turbulence and flux contributions over land and sea.

Over land, $kS_{w,u,v}(k)$ are about 3 times larger than over the tropical ocean in the inertial subrange (where the spectra display a $-2/3$ slope). Furthermore, $kS_w(k)$ shows a k^{-1} dependency at mesoscales ($4 \times 10^{-3} < k < 10^{-1}$) (i.e. a flat $S_w(k)$ spectrum) while $kS_{u,v}$ are flat. Over the tropical ocean, the mesoscale values of $S_{w,u,v}(k)$ relative to the inertial subrange are larger. This means that the spectra from the two regimes are not similar in shape, and that the mesoscale fluctuations, at least over the relatively homogeneous ocean, result from mesoscale processes rather than local turbulence generation by buoyancy and shear.

Cospectra of the vertical fluxes of both scalars and momentum show that on average the mesoscale contributions (wavenumbers $< 10^{-1}$ cycles km^{-1}) are insignificant. Of course, this does not mean that the mesoscale fluxes for individual cases are insignificant, only that on average they seem to cancel out. This is consistent with Sun et al. (1996).

These results provide useful guidance for estimating spectra of the three velocity components and scalars, and cospectra of these variables with vertical velocity in the convective boundary layer over both land and ocean.

Acknowledgements

NCAR is sponsored in part by the National Science Foundation.

REFERENCES

Britting, K. R., 1971: *Inertial Navigation Systems Analysis*, Wiley, New York, 249 pp.

Brown, E. N., C. A. Friehe, and D. H. Lenschow, 1983: The use of pressure fluctuations on the nose of an aircraft for measuring air motion, *J. Appl. Meteorol.*, **22**, 171–180.

Dobosy, R. J., T. L. Crawford, J. I. MacPherson, R. L. Desjardins, R. Kelly, S. P. Oncley, and D. Lenschow, 1997: Intercomparison among the four flux aircraft at BOREAS in 1994, *J. Geophys. Res.*, **102**, 29101–29111.

Johnson, R. H., P. E. Ciesielski, and J. A. Cotturone, 2001: Multiscale variability of the atmospheric mixed layer over the western Pacific warm pool, *J. Atmos. Sci.*, **58**, 2729–2750.

Kaimal, J. C. and J. J. Finnigan, 1994: *Atmospheric Boundary Layer Flows: Their Structure and Measurement*, Oxford University Press, New York, 81–83 pp.

Khelif, D., S. P. Burns, and F. C.A, 1999: Improved wind measurements on research aircraft, *J. Atmos. Oceanic Technol.*, **16**, 860–875.

Lenschow, D., 1972: The measurement of air velocity and temperature using the NCAR Buffalo aircraft measuring system, Technical Report NCAR-TN/EDD-74, National Center for Atmospheric Research.

Lenschow, D. and P. Spyers-Duran, 1989: *Measurement Techniques: Air Motion Sensing*, National Center for Atmospheric Research, Bulletin No. 23, available at: http://raf.atd.ucar.edu/Bulletins/bulletin23.html.

Lenschow, D. H., 1986: Aircraft measurements in the boundary layer, in *Probing the Atmospheric Boundary Layer*, edited by D. H. Lenschow, pp. 39–55, American Meteorological Society, Boston, MA.

NCAR, 1991: *Pressure Measurement from NCAR Aircraft*, National Center for Atmospheric Research, Bulletin No. 21, available on the web at: http://raf.atd.ucar.edu/Bulletins/bulletin21.html.

—, 2003: *The NSF/NCAR C-130Q Hercules (N130AR): Overview and Summary of Capabilities*, National Cntr. for Atmospheric Research, Bulletin No. 3, available at: http://raf.atd.ucar.edu/Bulletins/bulletin3.html.

Oncley, S. P., D. H. Lenschow, K. J. Davis, and T. L. Campos, 1997: Regional-scale surface flux observations across the boreal forest during BOREAS, *J. Geophys. Res.*, **102**, 29147–29154.

Sun, J., J. F. Howell, S. K. Esbensen, L. Mahrt, C. M. Greb, R. Grossman, and M. A. LeMone, 1996: Scale dependence of air-sea fluxes over the western equatorial Pacific, *J. Atmos. Sci.*, **53**, 2997–3012.

Williams, A., H. Kraus, and J. Hacker, 1996: Transport processes in the tropical warm pool boundary layer. part I: spectral composition of fluxes, *J. Atmos. Sci.*, **53**, 1187–1202.